JOC Article

Comparative Studies on the DNA-Binding Properties of Linear and Angular Dibenzoquinolizinium Ions

Heiko Ihmels,*,† Daniela Otto,† Francesco Dall'Acqua,‡ Anita Faccio,‡ Stefano Moro,‡ and Giampietro Viola‡

Organic Chemistry II, University of Siegen, Adolf-Reichwein-Str. 2, 57068 Siegen, Germany, and Department of Pharmaceutical Sciences, University of Padova, via Marzolo 5, I-35131 Padova, Italy

ihmels@chemie.uni-siegen.de

Received June 14, 2006

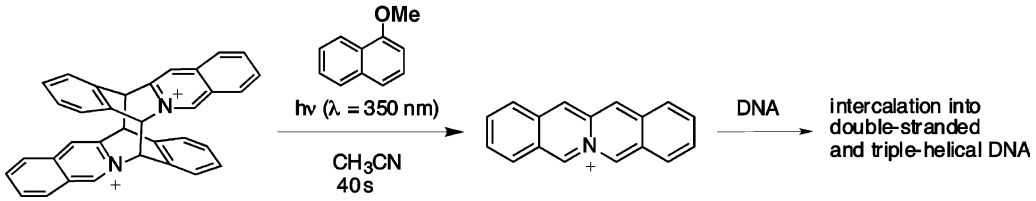

The interaction of the linear dibenzo[*b,g*]quinolizinium (**5a**) and the angular dibenzo[*a,f*]quinolizinium (**6**) with DNA was studied in detail in order to evaluate the influence of the shape of polycyclic quinolizinium ions on their DNA-binding properties. First, the synthesis and the thermally induced dimerization of **5a** were reinvestigated because the preparation and isolation of the bromide salt of **5a** according to literature procedures turned out to be problematic. The dibenzo[*b,g*]quinolizinium bromide [**5a(Br)**] tends to dimerize in solution with a highly selective and unprecedented formation of the corresponding *anti*-head-to-head dimer. Nevertheless, it was observed that careful exclusion of bromide ions from the reaction mixture suppresses the formation of the dimer. Moreover, the dimer may be transformed to the monomer by a remarkably rapid photoinduced electron-transfer reaction with 1-methoxynaphthalene. The association of **5a** and **6** with nucleic acids was investigated by spectrophotometric and spectrofluorimetric DNA titrations, CD and LD spectroscopy, DNA thermal denaturation studies, and competition-dialysis techniques. Both dibenzoquinolizinium ions **5a** and **6** exhibit an intercalative mode of binding to double-stranded DNA with moderate binding constants ($K = 1-7 \times 10^5$ M^{-1}) and a slight preference for association with GC-rich DNA regions. The structures of the intercalation complexes were calculated by molecular modeling methods. Competition-dialysis studies reveal that the isomers **5a** and **6** bind selectively to triple-helical DNA (poly[dA]-poly[dT]$_2$) as compared to selected synthetic and native double-stranded nucleic acids. Notably, the selectivity of the linear dibenzo[*b,g*]quinolizinium **5a** toward triplex DNA is higher than the one of the angular derivative **6**. In contrast, the DNA thermal denaturation studies reveal a higher stabilization of triple-helical DNA in the presence of **6** ($\Delta T_m^{3\rightarrow 2} = 28$ °C at $r = 0.5$) as compared to the stabilization by **5a** ($\Delta T_m^{3\rightarrow 2} = 14$ °C at $r = 0.5$). This comparison emphasizes the importance of the extended π system for the interaction of annelated quinolizinium ions with DNA. Moreover, the comparison between **5a** and **6** demonstrates the significant influence of the shape of the π system on the duplex- and triplex-stabilizing properties of the dibenzoquinolizinium ions.

Introduction

Benzo-annelated quinolizinium salts, such as coralyne (**1**), a well-known protoberberine derivative, and derivatives thereof represent an interesting class of compounds since they exhibit a high affinity for the association with DNA.[1] In the case of the protoberberines, this complex formation leads to topoisomerase poisoning in living cells and may, thus, be used to suppress the proliferation of unwanted cell tissue, such as tumor

† University of Siegen.
‡ University of Padova.

(1) Ihmels, H.; Faulhaber, K.; Vedaldi, D.; Dall'Acqua, F.; Viola, G. *Photochem. Photobiol.* **2005**, *81*, 1107.

10.1021/jo0612271 CCC: $33.50 © 2006 American Chemical Society
Published on Web 10/06/2006

CHART 1

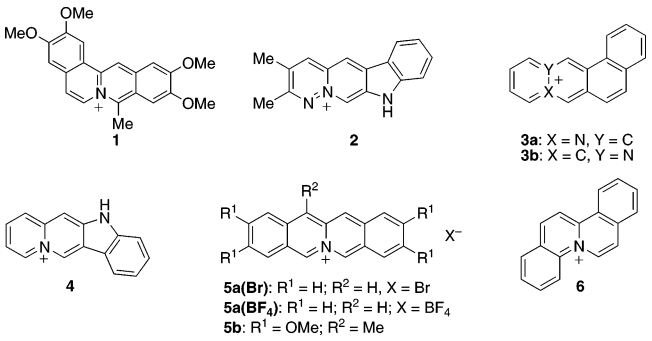

cells.[2] Moreover, a significant affinity for the association with triplex and quadruplex DNA was observed for coralyne.[3] To understand the parameters that govern the DNA-binding properties of annelated quinolizinium salts, related tetracyclic derivatives, such as **2**,[4] **3**,[5] and **4**,[6] have been investigated. Also, attempts have been made to synthesize and study the linearly annelated analogue of protoberberine, that is, derivatives of the dibenzo[*b*,*g*]quinolizinium ion (5a-azoniatetracene) (**5a**). During our studies of DNA-binding properties of annelated quinolizinium salts, we also intended to study the linear dibenzo[*b*,*g*]-quinolizinium (**5a**) as well as the angular, "S-shaped" isomer dibenzo[*a*,*f*]quinolizinium (**6**) to gain more knowledge on the influence of the shape of dibenzo-annelated quinolizinium ions on their DNA-binding properties. To exclude any substituent effect, which may interfere with the intended assessment of the shape-dependent properties, we focused our studies on the unsubstituted derivatives. Both compounds **5a** and **6** have been described previously; however, the investigation of the linear quinolizinium **5a** suffers from its rapid dimerization in solution. The parent compound was first synthesized by Bradsher et al.,[7] and a reversible thermal dimerization reaction of this compound to the formal product of a [4 + 4] cycloaddition has been reported. In addition, the derivative **5b** has been synthesized to study its antileukemic activity.[8] Although compound **5b** has been reported to be persistent toward dimerization,[9] a detailed analysis revealed its decomposition in solution and the formation of impurities due to dimerization.[8]

The cyclodimerization of **5a** has been reported to be induced by light, similar to dimerization reactions of anthracene[10] and benzo[*b*]quinolizinium derivatives.[11] Further photophysical studies on **5a** have shown that the dimers and the corresponding monomer may be reversibly interconverted upon irradiation.[12] In contrast, in a polymer matrix, a slow photodimerization along with a photopersistence of the dimer was reported.[13] Although the dimer structure has been proposed by several groups to be the one of the *anti*-head-to-tail dimer **aht-(5a)$_2$**, this structure assignment has not been proved by spectroscopic methods.

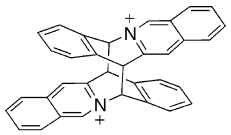

aht-(5a)$_2$

In this article, we present a comparative study of the DNA-binding properties of **5a** and **6**. We also demonstrate an efficient cycloreversion reaction to **5a** by a photoinduced electron-transfer process, along with the first structure assignment of the corresponding dimer.

Results and Discussion

Synthesis. The dibenzo[*a*,*f*]quinolizinium (**6**) was synthesized according to literature protocols.[14] We also attempted to synthesize **5a(Br)** according to a variation of the original literature procedure,[7] that is, cyclodehydration of the isoquinolinium salt **8(Br)** with hydrobromic acid. In contrast to the published procedure, the aldehyde functionality was protected as acetal instead of an aldoxime (Scheme 1).

Unfortunately, we were not able to isolate a pure sample of **5a(Br)** upon cyclodehydration with HBr because of its rapid dimerization, which is indicated by the bleaching of the initial red color of the solution and by the precipitation of a yellow solid. Attempts to isolate the monomer, for example, by immediate precipitation as tetrafluoroborate salt or by rapid evaporation of the solvent failed, as shown by ^{1}H NMR spectroscopic analysis. Nevertheless, it was possible to extract almost pure **5a(Br)** from the crude product with methanol (ca. 90% as determined by ^{1}H NMR spectroscopy) because the dimer is hardly soluble in this solvent. It may be noted, however, that even at these conditions, the dimer precipitates continuously from the methanol solution. Extended times for the cyclization reaction (12 h), keeping of the reaction mixture in the dark, or evaporation of the solvent yielded the dimer quantitatively. In contrast, the cyclization of the tetrafluoroborate salt **8(BF$_4$)** in polyphosphoric acid (PPA) gave the monomer **5a(BF$_4$)** in 73% yield without detectable traces of the dimer (Scheme 1). Unfortunately, the handling of **5a(BF$_4$)** is difficult because of its very low solubility in water and in polar organic solvents, such as acetonitrile, DMSO, or MeOH. For this reason, common ion metathesis,[15] that is, precipitation of a bromide or hydrogen sulfate from an acetonitrile solution of the tetrafluoroborate **5a-(BF$_4$)**, failed since the salt also precipitated under these conditions. Passing of **5a(BF$_4$)** through an ion-exchange resin also resulted in partial dimerization and decomposition to other unidentified products as indicated by ^{1}H NMR spectroscopic analysis.

(2) Palumbo, M.; Gatto, B.; Sissi, C. In *DNA and RNA Binders*; Demeunynck, M., Bailly, C., Wilson, W. D., Eds; Wiley-VCH: Weinheim, Germany, 2002; Chapter 19.
(3) (a) Lee, J. S.; Latimer, L. J. P.; Hampel, K. J. *Biochemistry* **1993**, *32*, 5591. (b) Moraru-Allen, A. A.; Cassidy, S.; Asensio Avarez, J.-L.; Fox, K. R.; Brown, T.; Lane, A. N. *Nucleic Acids Res.* **1997**, *25*, 1890. (c) Franceschin, M.; Rosetti, L.; D'Ambrosio, A.; Schirripa, S.; Bianco, A.; Ortaggi, G.; Savino, M.; Schultes, C.; Neidle, C. *Bioorg. Med. Chem. Lett.* **2006**, *16*, 1707.
(4) Molina, A.; Vaquero, J. J.; Garcia-Navio, J. L.; Alvarez-Builla, J.; de Pascual-Teresa, B.; Gado, F.; Rodrigo, M. M. *J. Org. Chem.* **1999**, *64*, 3907−3915.
(5) Viola, G.; Bressanini, M.; Gabellini, N.; Dall'Acqua, F.; Vedaldi, D.; Ihmels, H. *Photochem. Photobiol. Sci.* **2002**, *11*, 882.
(6) (a) Ihmels, H.; Bringmann, G.; Faulhaber, K.; Messer, K.; Sturm, C.; Vedaldi, D.; Viola, G. *Eur. J. Org. Chem.* **2001**, *6*, 1157. (b) Viola, G.; Dall'Acqua, F.; Gabellini, N.; Moro, S.; Vedaldi, D.; Ihmels, H. *ChemBioChem* **2002**, *3*, 101.
(7) Bradsher, C. K.; Solomons, T. W. G. *J. Am. Chem. Soc.* **1960**, *82*, 1808.
(8) Zee-Cheng, R. K. Y.; Cheng, C. C. *J. Med. Chem.* **1976**, *19*, 883.
(9) Wiegrebe, W.; Sasse, D.; Roesel, E. *Arch. Pharm.* **1968**, *301*, 33.
(10) Bouas-Laurent, H.; Castellan, A.; Desvergne, J.-P.; Lapouyade, R. *Chem. Soc. Rev.* **2000**, *29*, 43.
(11) Lehnberger, C.; Scheller, D.; Wolff, T. *Heterocycles* **1997**, *10*, 2033.
(12) Bendig, J.; Bauer, U.; Kreysig, D. *Z. Phys. Chem.* **1981**, *262*, 1041.
(13) Tomlinson, W. J.; Chandross, E. A.; Fork, R. L.; Pryde, C. A.; Lamola, A. A. *Appl. Opt.* **1972**, *11*, 533.
(14) Fozard, A.; Bradsher, C. K. *J. Org. Chem.* **1966**, *31*, 3683.
(15) Gries, W.-K.; Günther, E.; Hünig, S. *Liebigs Ann.* **1991**, 1021.

SCHEME 1

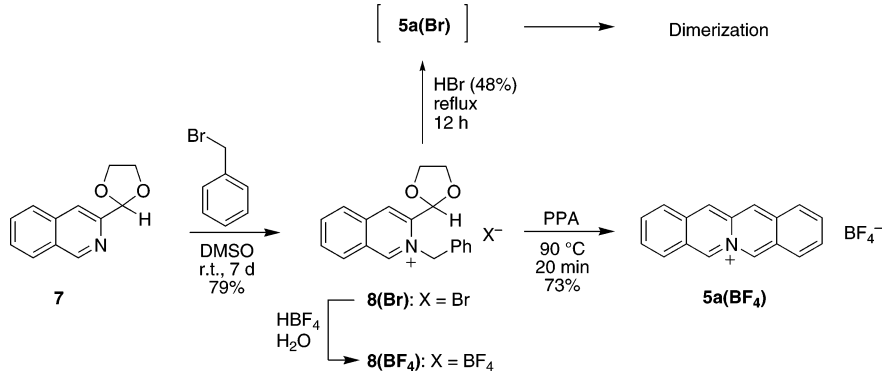

The good yield of **5a(BF$_4$)** by efficient suppression of dimer formation in the cyclization with tetrafluoroborate as counterion led us to the assumption that the bromide ion may play a crucial role in the ground-state dimerization of **5a** when the cyclization is performed with **8(Br)**. Further evidence for this proposal was obtained, as the addition of bromide ions (as aqueous NaBr solution or aqueous hydrobromic acid) to **5a(BF$_4$)**, which is otherwise persistent, led to dimerization as monitored by ^{1}H NMR spectroscopy.

The structural assignment of the dimer of **5a** was made on the basis of chemical shifts and signal patterns of the bridgehead protons in the ^{1}H NMR spectrum, as already described for benzo-annelated quinolizinium salts, namely, acridizinium derivatives, whose photodimerization in solution and in the solid state is well-known.[5] Most significantly, only one set of signals, whose assignment was based on additional 2D NMR experiments, was observed at 600 MHz (cf. Supporting Information). Moreover, the bridgehead protons at C-12 give one singlet at 6.02 ppm. Both observations reveal that only one of the four possible dimers has formed. Also, symmetry considerations indicate a head-to-head dimer because a head-to-tail dimer would result in a doublet instead of a singlet for the bridgehead protons, with a characteristic coupling constant of $J = 11$ Hz. In addition, ROESY-NMR experiments showed a NOE interaction between the proton pairs 5-H/8′−H and 11-H/13′−H, indicating a *syn* orientation of the aromatic moieties (cf. Supporting Information). Thus, the dimer structure could be assigned to **ahh-(5a)$_2$**.

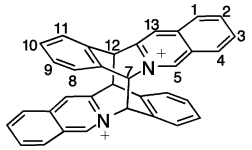

ahh-(5a)$_2$

The structural assignment of the dimer indicates a remarkable selectivity of the dimerization process, compared with the one of structurally related acridizinium salts (benzo[*b*]quinolizinium).[16] In the absence of directional or topological effects, such as in the solid state,[17] photodimerizations of benzo[*b*]-quinolizinium ions usually yield all four possible dimers upon irradiation with a slight preference for the head-to-tail dimers. Although there are no sufficient data available to deduce the reaction mechanism, we assume that the selectivity in the dimerization of **5a** is caused by a different reaction mechanism as compared to the [4 + 4] photocycloaddition, especially since the addition of bromide ions to the monomer **5a** leads to a dimerization to **ahh-(5a)$_2$**. Most likely a radical- or ion-induced stepwise mechanism takes place. Nevertheless, further detailed studies that are required to elucidate the dimerization mechanism are almost impossible because the low solubility of the dimer and the monomer interferes with detailed quantitative spectroscopic analyses.

The efficient dimerization of the dibenzoquinolizinium **5a** turned out to be a significant problem that prevented its further investigation. Therefore, attempts were made to transform the dimer to the monomer by thermolysis or photolysis, as it is known that dimers of anthracene and derivatives thereof may be transformed to the corresponding monomers.[18] Although both methods have been reported to give **5a** from the corresponding dimer, neither of these methods yielded detectable amounts of dibenzo[*b,g*]quinolizinium **5a** in our hands. The dimer **ahh-(5a)$_2$** was heated under reflux in ethanol or acetic acid for 12 h, respectively, but the analysis of the reaction mixture by ^{1}H NMR spectroscopy showed not even traces of the monomer. The irradiation of the dimer **ahh-(5a)$_2$** at $\lambda > 320$ nm did not give the monomer, either. It should be considered that both monomer and dimer absorb at the applied wavelengths, so that a photodimerization may also be induced under these conditions. However, according to the data from Bradsher et al.,[6] the dimer has an almost identical extinction coefficient as the monomer at $\lambda = 366$ and 355 nm, that is, at the emission maxima of the employed lamps, so that a photostationary equilibrium should be established. Also, it should be noted that a cycloreversion of the dimer has been reported to take place upon irradiation of the dimer in dichloromethane at $\lambda = 365$ nm.[12] In contrast, we were not able to dissolve sufficient amounts of the dimer in dichloromethane, so that we could not reproduce these results.

Since it is known that cycloreversions are also achieved by photoinduced electron-transfer (PET) processes,[19] it was investigated whether the dimer **ahh-(5a)$_2$** may be cleaved by this method. As the quinolinium moiety of the dimer **ahh-(5a)$_2$**

(16) Ihmels, H.; Mohrschladt, C. J.; Schmitt, A.; Bressanini, M.; Leusser, D.; Stalke, D. *Eur. J. Org. Chem.* **2002**, 2624.

(17) (a) Wang, W. N.; Jones, W. *Tetrahedron* **1987**, *43*, 1273. (b) Kearsley, D. K. In *Organic Solid State Chemistry*; Desiraju, G. R., Ed.; Elsevier: Amsterdam, 1987; p 69. (c) Ihmels, H.; Leusser, D.; Pfeiffer, M.; Stalke, D. *J. Org. Chem.* **1999**, *64*, 5715.

(18) Bouas-Laurent, H.; Castellan, A.; Desvergne, J.-P.; Lapouyade, R. *Chem. Soc. Rev.* **2001**, *29*, 248.

(19) (a) Barber, R. A.; de Mayo, P.; Okada, K.; Wong, S. K. *J. Am. Chem. Soc.* **1982**, *104*, 4995. (b) Masnovi, J. M.; Kochi, J. K. *J. Am. Chem. Soc.* **1985**, *107*, 6781. (c) Mitzner, R.; Bendig, J.; Kreysig, D. *Z. Chem.* **1986**, *26*, 255. (d) Ihmels, H.; Mohrschladt, C. J.; Schmitt, A.; Bressanini, M.; Leusser, D.; Stalke, D. *Eur. J. Org. Chem.* **2002**, 2624.

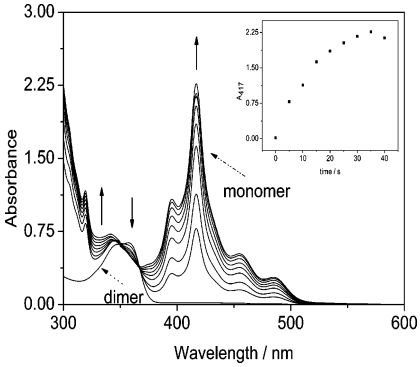

FIGURE 1. Photoinduced conversion of **ahh-(5a)$_2$** ($c = 10^{-4}$ M) into the corresponding monomer **5a** in the presence of 1-methoxynaphthalene ($c = 2 \times 10^{-3}$ M); in phosphate buffer (pH = 7.0), $\lambda_{ex} = 350$ nm. Inset: time-dependent increase of the absorption band at $\lambda = 417$ nm.

should exhibit considerable electron-acceptor properties, a photoinduced electron transfer between the dimer and an appropriate donor molecule may lead to a cycloreversion reaction. In fact, the irradiation of **ahh-(5a)$_2$** and 1-methoxynaphthalene in aqueous buffer solution for only 40 s led to the formation of the monomer almost quantitatively. The formation of **5a(Br)** during irradiation was monitored by absorption spectroscopy (Figure 1). After 35 s, the absorption of the monomer reached its maximum, indicating the formation of maximum amount of the monomer, whereas after 40 s, the absorption decreased, which reveals a secondary decomposition pathway of **5a**. An energy transfer from the excited 1-methoxynaphthalene to the dimer **ahh-(5a)$_2$** can be excluded because the reaction takes place also when irradiated at $\lambda > 335$ nm. In this wavelength region, the dimer still absorbs, but not the 1-methoxynaphthalene (cf. Supporting Information). We compared the absorption spectra of **5a(Br)** with the one given in the literature by Bendig and Helm[20] and determined an extinction coefficient of $\epsilon_{417} = 22.7 \times 10^3$ L mol^{-1} cm^{-1}, which is slightly larger than the one taken from reported spectra ($\epsilon_{417} = 19.4 \times 10^3$ L mol^{-1} cm^{-1}).

Association of 5a and 6 with Double-Stranded DNA. With the above-mentioned methods, sufficient amounts of **5a(Br)** and **5a(BF$_4$)** were available for further studies of their interaction with DNA. Thus, **5a(BF$_4$)** was obtained by direct synthesis according to Scheme 1; however, the use of this compound is limited due to its low solubility in water. For experiments with the water-soluble salt **5a(Br)**, a solution of the dimer **ahh-(5a)$_2$** and 1-methoxynaphthalene in water was irradiated for 40 s, and the naphthalene was removed by extraction with dichloromethane. The aqueous phase was analyzed by absorption spectroscopy and used as solution of **5a(Br)** that was employed immediately for further experiments, such as the spectrophotometric titration with calf thymus DNA. Nevertheless, **5a(Br)** decomposes rapidly upon standing in solution, even in the dark (cf. Supporting Information).

The addition of calf thymus DNA (ct DNA) to a solution of **5a(Br)** or **6** resulted in a significant bathochromic shift of the absorption maxima, along with a decrease of the signal intensity in both cases (Figure 2A,B). Similar titration curves were obtained upon addition of the synthetic heteropolynucleotides (poly[dA-dT]-poly[dA-dT]) and (poly[dG-dC]-poly[dG-dC]) to quinolizinium derivatives **5a** and **6** (cf. Supporting Information).

(20) Bendig, J.; Helm, S. *Z. Chem.* **1990**, *9*, 326.

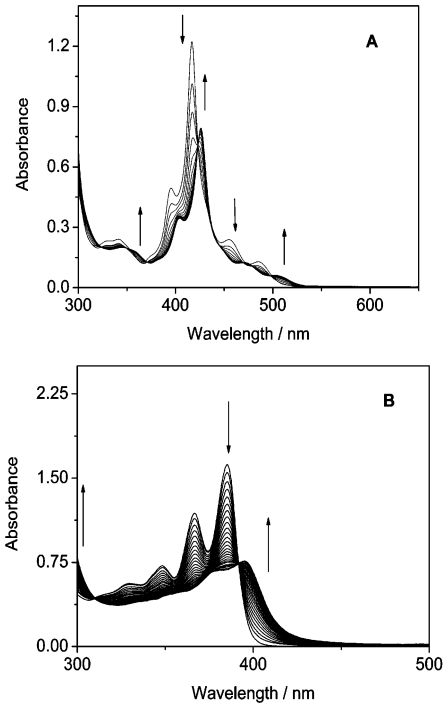

FIGURE 2. Spectrophotometric titration of ct DNA to dibenzoquinolizinium ions **5a** (A) and **6** (B) in phosphate buffer (0.01 M, pH 7.0, $T = 25$ °C; $c = 10^{-4}$ mol/L); arrows indicate the development of the absorption bands upon DNA titration.

Such a perturbation of the absorption spectra on DNA addition usually indicates the strong association of the cationic ligand with DNA.[1,21] Most notably, isosbestic points appear at the beginning of each titration, that is, at small ligand-to-DNA ratios, r (**5a**: $r < 0.13$; **6**: $r < 0.2$; ratios with respect to molar equivalents, DNA concentration always in bases), which indicate that one type of quinolizinium−DNA complex is formed preferentially. Upon increasing the DNA-to-ligand ratio, however, the isosbestic points disappear, which may be a sign for an additional binding mode that is adopted under these conditions. In addition, the analysis of the spectrophotometric titrations according to McGhee and van Hippel[22] was used to determine the association constant (K) and the binding size (n) between the ligand and the nucleic acids. The data are collected in Table 1, along with the reported binding constants of the monobenzo-annelated quinolizinium ion **9**[23] and coralyne (**1**).[24] The binding constants K reveal high binding affinities of **5a** ($K = 1.2 \times 10^5$ M^{-1}) and **6** ($K = 1.9 \times 10^5$ M^{-1}) to ct DNA that are comparable to the one of coralyne (**1**), that is, a known intercalator with dibenzoquinolizinium structure. Whereas the derivative **5a** has essentially the same values for the binding constants with all three nucleic acids, the derivative **6** exhibits slightly larger binding constants with (poly[dA-dT]-poly[dA-dT]) and (poly[dG-dC]-poly[dG-dC]). The latter data are in good agreement with the ones of coralyne (**1**), which have been used to deduce a GC-selective binding of the latter.[24] It is also

(21) Cantor, C. R.; Schimmel, P. R. In *Biophysical Chemistry Part 2: Techniques for the Study of Biological Structure and Function*; Freeman: New York, 1980; p 444.

(22) McGhee, J. D.; von Hippel, P. H. *J. Mol. Biol.* **1974**, *86*, 469.

(23) Ihmels, H.; Faulhaber, K.; Sturm, C.; Bringmann, G.; Messer, K.; Gabellini, N.; Vedaldi; D.; Viola, G. *Photochem. Photobiol.* **2001**, *74*, 505.

(24) Pal, S.; Suresh Kumar, G.; Debnath, D.; Maiti, M. *Ind. J. Biochem. Biophys.* **1998**, *35*, 321.

TABLE 1. Binding Constants and Binding-Site Size of Dibenzoquinolizinium Derivatives 5a and 6, Benzo[*b*]quinolizinium Bromide (9), and Coralyne (1) as Determined from Spectrophotometric Titrations with ct DNA, (poly[dA-dT]-poly[dA-dT]), and (poly[dG-dC]-poly[dG-dC])

	ct DNA		(poly[dG-dC]-poly[dG-dC])		(poly[dA-dT]-poly[dA-dT])	
	$K^a \times 10^{-5}$ (M^{-1})	n^a/bases	$K^a \times 10^{-5}$ (M^{-1})	n^a/bases	$K^a \times 10^{-5}$ (M^{-1})	n^a/bases
5a	1.2	2	1.3	2	1.6	2
6	1.9	3	6.9	4	3.0	4
1[d]	1.0	9	9.8	4	6.4	7
9[b]	0.2[c]	6[c]	0.6	4	0.1	9

[a] *K* is the binding constant (in bases), and *n* is the binding-site size. [b] From ref 23. [c] Determined for st DNA. [d] From ref 24; in BPES buffer (pH 7.0) containing 30% (v/v) ethanol.

demonstrated that—such as for other intercalators—the extension of the π system is a key parameter that determines the strength of the DNA association because the binding constants of **5a** and **6** are 1 order of magnitude larger than the one of **9**; the latter has a significantly smaller π system than **5a** and **6**. The binding-site size *n* of the dibenzo[*a*,*f*]quinolizinium **6** is 4 (in bases), which is in agreement with an intercalative binding mode, whereas the binding-site size of **5a** is 2, which is too small for intercalation (according to the neighbor-exclusion model) and groove binding. Thus, a binding-site size of 2 may indicate additional π stacking of the ligand along the DNA backbone, especially at low DNA-to-ligand ratios.

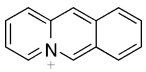

9

For the evaluation of the effect of the ligand association on the DNA stability, thermal denaturation experiments were performed with ct DNA and double-stranded poly[dA-dT]-poly[dA-dT] at different ligand-to-DNA ratios *r* (Figure 3). Unfortunately, in the case of derivative **5a**, these experiments were disturbed by the decomposition of **5a** at elevated temperatures (cf. Supporting Information) that leads to a significant decrease of the ligand absorption. Nevertheless, the melting profiles could be used to determine the melting temperature of the nucleic acids in the presence of ligand **5a**. Even at low ionic strength [$c(Na^+) = 16$ mM], the linear dibenzoquinolizinium **5a** has only a small effect on the stabilization of double-stranded nucleic acids as shown by the small increase of the DNA melting temperatures (ct DNA: $\Delta T_m = 6$ °C at $r = 0.5$; poly[dA-dT]-poly[dA-dT]: $\Delta T_m = 10$ °C at $r = 0.5$). The angular dibenzoquinolizinium **6** has a more pronounced stabilizing effect on the duplex DNA under identical conditions (ct DNA: $\Delta T_m = 13$ °C at $r = 0.5$; poly[dA-dT]-poly[dA-dT]: $\Delta T_m = 20$ °C at $r = 0.5$). The complete data set is summarized in Table 2. These data reveal a difference between the two dibenzoquinolizinium isomers **5a** and **6** with respect to their DNA-stabilizing properties. Thus, double-stranded DNA is significantly stabilized by the angular dibenzoquinolizinium **6**, whereas the stabilization of the DNA double helix by the linear analogue **5a** is rather weak. Apparently, the corresponding DNA single strand is also significantly stabilized by **5a**. For comparison, the stabilization of double-stranded DNA by **6** is essentially the same as the one by coralyne (**1**) (ct DNA: $\Delta T_m = 9$ °C at ligand-to-DNA ratio $r = 0.1$; poly[dA-dT]-poly[dA-dT]: $\Delta T_m = 7$ °C at $r = 0.1$).[24] Moreover, upon association with the monobenzo-annelated quinolizinium **9**, the double-stranded DNA is only stabilized marginally, as indicated by a minimal increase of the melting temperature (ct DNA: $\Delta T_m = 3$ °C at $r = 0.5$; poly-[dA-dT]-poly[dA-dT]: $\Delta T_m = 4$ °C at $r = 0.5$; cf. Supporting Information). This comparison underlines again the importance of the extended π system for the interaction of annelated quinolizinium ions with DNA. Moreover, the comparison between **5a** and **6** shows that the shape of the π system also has a significant impact on the duplex-stabilizing properties of the dibenzoquinolizinium ions.

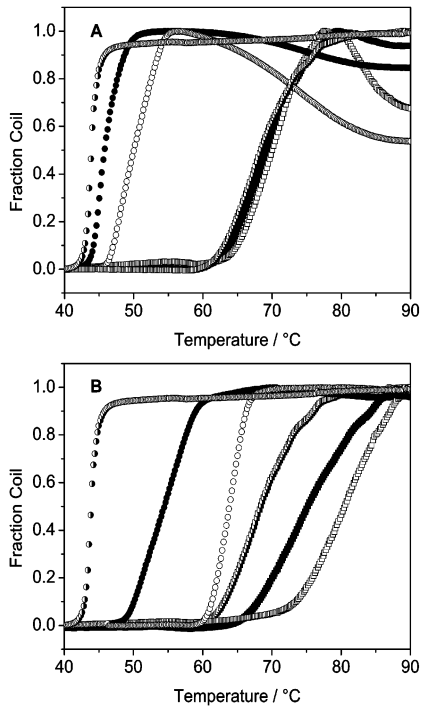

FIGURE 3. Melting profiles of poly[dA-dT]-poly[dA-dT] (circles) and calf thymus DNA (squares) in the presence of dibenzo[*b*,*g*]-quinolizinium tetrafluoroborate (**5a**) (A) and dibenzo[*a*,*f*]quinolizinium tetrafluoroborate (**6**) (B) at ligand-to-DNA ratios of 0 (half filled circles and squares), 0.2 (filled circles and squares), and 0.5 (open circles and squares); c(DNA) = 40 μM (bp) in BPE buffer.

To gain more information on the binding mode of the dibenzoquinolizinium derivatives **5a** and **6**, the LD and CD spectra of solutions of **5a(BF$_4$)** or **6** with varying amounts of DNA were determined in a flow cell (Figure 4). Without DNA, no LD signal was observed, but upon addition of salmon testes DNA (st DNA), a negative LD signal develops in the wavelength range, in which only the ligands absorb (i.e., between 350 and 500 nm). In both cases, the negative LD signal of the DNA bases at $\lambda \approx 260$ nm increases with higher ligand-to-DNA ratios, which usually indicates the stiffening of the DNA due to intercalation of the ligand. Moreover, the reduced LD signals of the DNA and of the bound ligands are almost identical, and the LD absorption of the ligand is independent of the wavelength, which reflects a single binding mode at these

TABLE 2. Induced Change of Melting Temperature (in °C) of Double-Stranded and Triplex DNA upon Association of 5a, 6, and 9 Derived from Thermal Denaturation Studies[a]

	ds DNA[b]				poly(dA)-poly(dT)$_2$[c]									
	ct DNA		(poly[dA-dT]-poly[dA-dT])		$\Delta T_m^{3\rightarrow2}$					$\Delta T_m^{2\rightarrow1}$				
r	0.2	0.5	0.2	0.5	0.1	0.2	0.3	0.4	0.5	0.1	0.2	0.3	0.4	0.5
5a	4	6	5	10	1	4	7	11	14	<1	<1	<1	1	<1
6	7	13	11	20	13	15	23	26	28	<1	1	1	1	1
9	2	3	2	4	<1	1	<1	1	1	<1	1	<1	<1	<1

[a] Experimental conditions: $c_{DNA} = 40\ \mu M$ in bp or bt; estimated error ±1 °C. [b] In BPE buffer, $c_{Na+} = 16$ mM. [c] In BPES buffer, $c_{Na+} = 200$ mM.

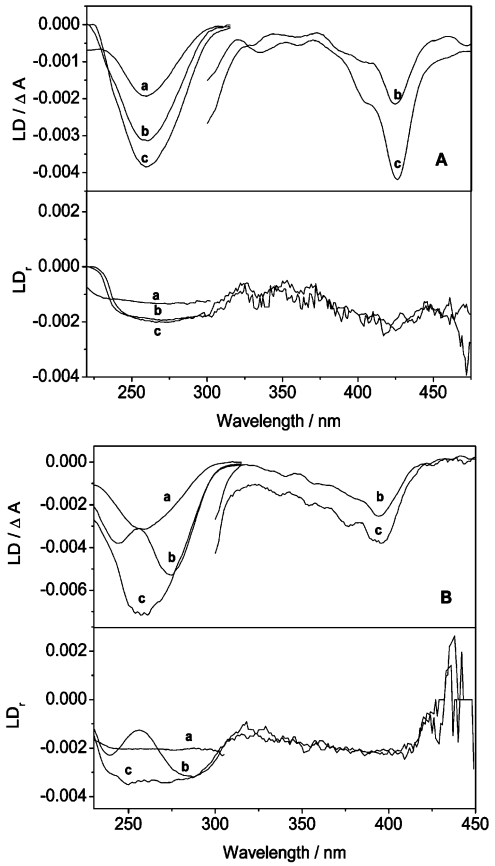

FIGURE 4. Linear dichroism (LD) and reduced linear dichroism (LDr) spectra of compounds **5a** (A) and **6** (B) recorded in ETN buffer, 0.01 M, pH = 7.0; ligand-to-DNA ratios: $a = 0.0$, $b = 0.08$, and $c = 0.2$; c(DNA) = 2.27 mM in bases.

particular DNA-to-ligand ratios. Altogether, the data from the LD spectroscopic investigations show that both dibenzoquinolizinium ions **5a** and **6** intercalate into double-stranded DNA at the employed DNA-to-ligand ratios.

Notably, the CD spectrum of a mixture of quinolizinium **5a** and st DNA does not show a CD signal for the DNA-bound ligand (Figure 5A), which was rather unexpected since a nondegenerative coupling between the DNA and the bound ligand usually results in an induced CD (ICD) for the ligand.[25] On the other hand, the slight increase of the CD signal intensity of the DNA bases indicates the interaction between **5a** and the nucleic acid. As all other binding studies confirm the association of **5a** with DNA (Table 1), the absence of an ICD signal of the bound quinolizinium may indicate that the aromatic compound intercalates only partly in DNA, such as, for example, coralyne,

(25) Nordén, B.; Kurucsev, T. *J. Mol. Recognit.* **1994**, *7*, 141.

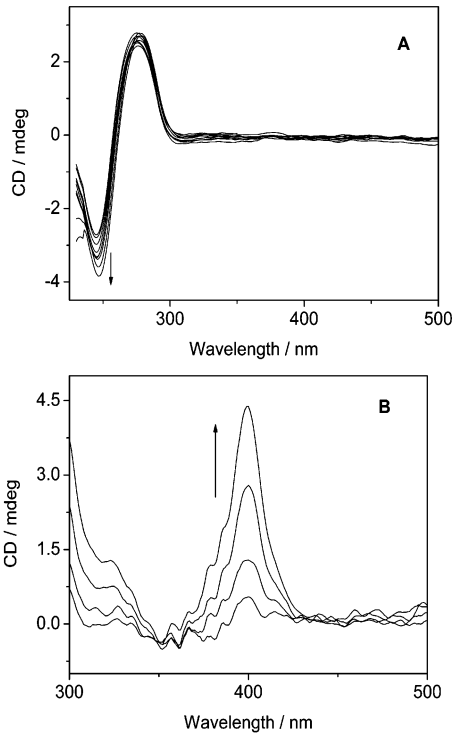

FIGURE 5. Circular dichroism (CD) spectra of compounds **5a** (A) and **6** (B) recorded in ETN buffer, 0.01 M, pH = 7.0, at different ligand-to-DNA ratios; arrows indicate the development of the CD bands upon DNA titration.

and that this binding mode only leads to a weak coupling between the transition dipole of the quinolizinium chromophore and the ones of DNA. In contrast, a significant positive ICD signal appears in the long-wavelength absorption range of dibenzoquinolizinium **6** upon addition of DNA. For an intercalated compound, a positive ICD signal indicates an orientation of the transition dipole perpendicular to the long axis of the binding pocket. As AM1 calculations reveal a transition dipole moment μ_1 of the long-wavelength absorption as shown in Figure 6, it can be deduced that ion **6** intercalates into ds DNA such that the isoquinolinium moiety of **6** is oriented almost parallel to the long axis of the intercalation pocket (Figure 6).

Molecular Modeling Studies. Molecular modeling studies support the above presented experimental evidence that both dibenzoquinolizinium ions **5a** and **6** may intercalate into DNA (Figure 7, cf. Supporting Information). The theoretical energies of intercalation suggest that the dibenzoquinolizinium ion **5a** might be slightly more effective as intercalator than the derivative **6** in both AT and GC intercalation sites [AT site: $\Delta E_{interc.} = -12.3$ kcal/mol (**5a**), $\Delta E_{interc.} = -11.6$ kcal/mol (**6**); GC site: $\Delta E_{interc.} = -12.6$ kcal/mol (**5a**) vs −11.8 kcal/mol (**6**)].

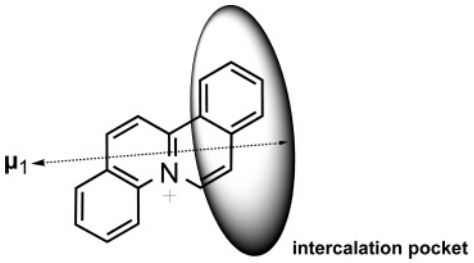

FIGURE 6. Transition dipole moment of **6** as calculated by AM1 (μ_1 of the long-wavelength absorption $\lambda = 387$ nm) and possible orientation of **6** relative to the DNA intercalation site as deduced from CD spectroscopy.

Nevertheless, as compared to the linear derivative **5a**, the angular shape of the dibenzoquinolizinium ion **6** allows a relatively large area of overlap between the intercalator and the two DNA base pairs that constitute the intercalation pocket; that is, one naphthalene moiety of **6** is accommodated in the intercalation site with the other naphthalene part pointing inside the groove. The calculated binding geometry is in agreement with the CD spectroscopic results. In contrast, the derivative **5a** is too long to completely fit into the intercalation site. As a consequence, this compound intercalates with its long molecular axis perpendicular to the long axis of the binding site and, thus, establishes a weaker π stacking between the intercalated planar aromatic system and the DNA bases (Figure 7). The inconsistency between the slightly higher energy of intercalation and the lower stacking interaction of dibenzoquinolizinium ion **5a**—as compared to **6**—demonstrates that the overall energy of intercalation is not solely governed by the stacking interactions between intercalator and DNA bases.[26] Notably, several other factors, such as hydrogen bonding, van der Waals stacking, Lewis acid−base interactions, dipole−dipole interactions, as well as conformational changes of the DNA and the extent of counterion release, contribute significantly to the overall binding energy. Presumably, the calculations also consider additional contributions, presumably dispersive van der Waals interactions, that result from the accommodation of the nonintercalated part of the dibenzoquinolizinium **5a** in the groove.

Competition-Dialysis Assay. To assess whether the dibenzoquinolizinium ions **5a** and **6** exhibit a pronounced binding selectivity for a particular nucleic acid, competition-dialysis experiments were carried out.[27] Selected DNA samples were dialyzed against a mutual stock solution of **5a(BF$_4$)** or **6**, and the relative amount of the bound ligand was determined by absorption spectroscopy (Figure 8). These experiments allow one to determine the relative affinity of **5a** and **6** toward the employed DNA samples. The data reveal that **5a** and **6** bind with a slight preference in GC-rich nucleic acids, such as *Micrococcus luteus* DNA (ml DNA, GC = 72%) and (poly[dG-dC]-poly[dG-dC]) as compared to ct DNA (GC = 42%) and (poly[dA-dT]-poly[dA-dT]). This observation is in agreement with the photometric titrations that reveal slightly higher binding constants for the association of **6** with (poly[dG-dC]-poly[dG-dC]) as compared to the ones obtained for (poly[dA-dT]-poly[dA-dT]). Nevertheless, the binding preferences of **5a** that are determined by the competition-dialysis method do not match the trend of the binding constants obtained from photometric titrations (Table 1). Presumably, this indicates a rather large intrinsic error in the binding constants as they are derived from a fit of the experimental data to a multiexponential function, in which even small deviations result in large changes of the resulting binding constant, *K*, and the binding-site size, *n*. These results also demonstrate that binding constants from photometric titrations should not be used as the only criterion to analyze binding selectivities.

Most notably, a high binding affinity to triplex DNA, such as poly(dA)-poly(dT)$_2$, was observed for compound **5a**. Thus, its affinity to triplex DNA is approximately 10-fold larger than the one toward ct DNA. This tendency for triplex binding may also be the reason for the observation that **5a** binds to polydA-polydT even with a slightly higher selectivity than to (poly[dG-dC]-poly[dG-dC]) because polydA-polydT tends to disproportionate to polydT and poly(dA)-poly(dT)$_2$ in the presence of triplex binders. The angular dibenzoquinolizinium ion **6** also exhibits a clear preference for triplex DNA binding; however, the selectivity is not as pronounced as in the case of **5a**. For comparison, the monobenzo-annelated quinolizinium **9** does not

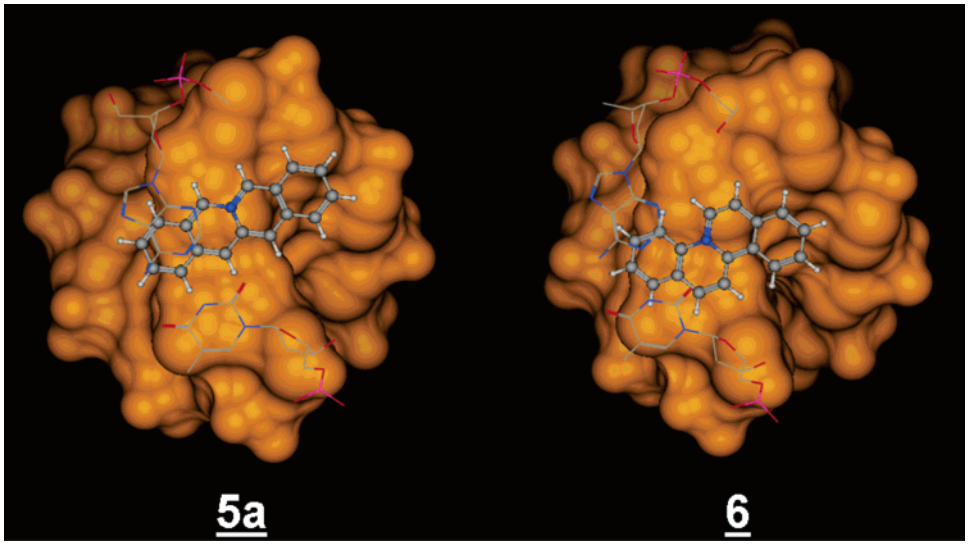

FIGURE 7. Optimized geometries of the intercalation complexes (AT sites) of dibenzoquinolizinium ions **5a** and **6** with ds DNA as obtained by molecular docking simulations (see Experimental Section for details); ds DNA is represented by its Connolly's surface.

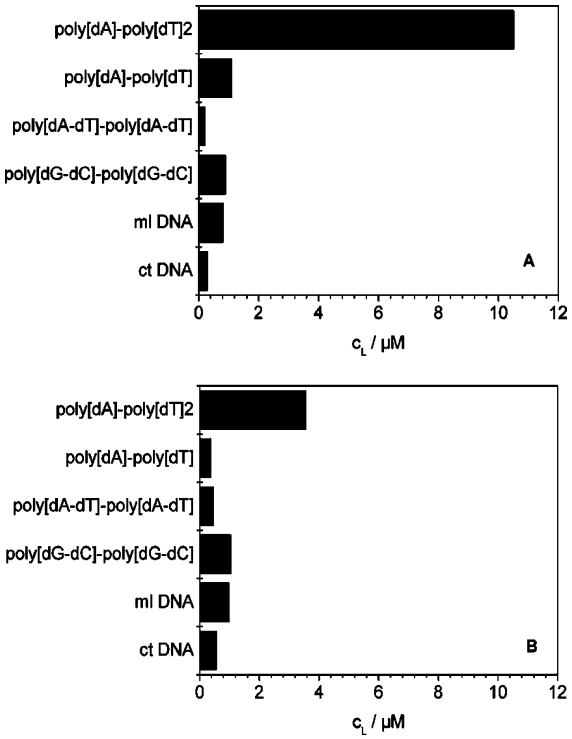

FIGURE 8. Competition-dialysis data for dibenzo[*b*,*g*]quinolizinium tetrafluoroborate (**5a**) (A) and dibenzo[*a*,*f*]quinolizinium tetrafluoroborate (**6**) (B) in BPES buffer. Data are presented as a bar graph in which the amount of ligand bound to each nucleic acid structure is plotted.

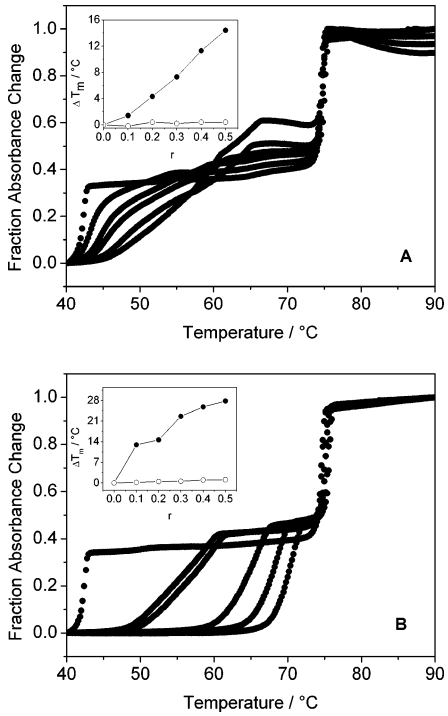

FIGURE 9. Melting profiles of poly[dA]-poly[dT]$_2$ in the presence of dibenzo[*b*,*g*]quinolizinium (**5a**) (A) and dibenzo[*a*,*f*]quinolizinium (**6**) (B) at ligand-to-DNA ratios of 0, 0.1, 0.2, 0.3, 0.4, and 0.5 (r); c(DNA) = 40 μM (bt) in BPES buffer. Insets show the dependence of T_m shifts ($\Delta T_m^{3\rightarrow2}$: filled circles; $\Delta T_m^{2\rightarrow1}$: open circles) on the ligand-to-DNA ratio.

exhibit a significant selective binding to triplex DNA (cf. Supporting Information).

Stabilization of Triplex DNA by 5a and 6. The results from the competition-dialysis experiments reveal a selective association of the dibenzoquinolizinium derivatives **5a** and **6** with triplex DNA, at least as compared to the other employed double-stranded nucleic acids. Therefore, the interaction of the dibenzoquinolizinium ions **5a** and **6** with triple-helical DNA was further studied by thermal denaturation experiments of the triplex DNA in the presence of these ligands (Figure 9 and Table 2). In the case of **5a**, however, the decomposition of this compound was again indicated by a significant fluctuation of the absorption at higher temperatures (cf. Supporting Information). The stabilization of triple-helical DNA by the association with **5a** or **6** was investigated by thermal denaturation of poly(dA)-poly(dT)$_2$ at high ionic strength [c(Na$^+$) = 200 mM]. At these conditions, attractive ionic interactions are significantly reduced, and the melting temperature of double-stranded DNA is not increased upon addition of the ligand (cf. Supporting Information). However, under these conditions, the triple-helical DNA is significantly stabilized in the presence of **5a** and **6** as shown by an increase of the melting temperature $T_m^{3\rightarrow2}$ that indicates the dissociation of the triplex to one single strand and the duplex (**5a**: $\Delta T_m^{3\rightarrow2}$ = 14 °C at r = 0.5; **6**: $\Delta T_m^{3\rightarrow2}$ = 28 °C at r = 0.5). At this ligand-to-DNA ratio, the stability of the duplex DNA is not influenced ($\Delta T_m^{2\rightarrow1} \leq 1$ °C).

Notably, the triplex DNA is stabilized to a higher extent upon association with dibenzoquinolizinium **6** as compared to the derivative **5a**. In fact, the triplex-stabilizing properties of **6** are comparable to the ones of the well-established naphthylquinolines[28] that exhibit similar triplex-melting temperatures under almost identical conditions, and thus **6** represents one of the few examples of triplex-stabilizing ligands that do not require additional aminoalkyl substituents for efficient binding.[29] Notably, in contrast to dibenzoquinolizinium **6**, some naphthylquinolines also stabilize the duplex DNA ($\Delta T_m^{2\rightarrow1} \approx 5$ °C at r = 0.2).[28a] Thus, compound **6** exhibits even a more pronounced selectivity for triplex stabilization as compared to these naphthylquinoline derivatives. The significant stabilization of the triplex DNA by the dibenzoquinolizinium **6** may be rationalized with the help of the structure of the intercalation complex (Figure 7). Thus, upon intercalation of **6**, one azonianaphthalene moiety points inside the DNA groove and provides a connection point for the third DNA strand. Most likely the single strand associates to the already bound dibenzoquinolizinium by intercalative interactions. In the case of dibenzoquinolizinium **5a**, a similar connection with the aromatic part that points outside the intercalation site in the ds DNA may be possible. Nevertheless, as the linear shape of the molecule cannot match the helical structure of the resulting triplex, a lower degree of stabilization takes place upon triplex formation as compared to **6**. The requirement of the tetracyclic π system is supported by the

(26) For a detailed discussion see: (a) Ren, J.; Jenkins, T.; Chaires, J. B. *Biochemistry* **2000**, *39*, 8439. (b) Reha, D.; Kabelac, M.; Ryjacek, F.; Sponer, J.; Sponer, J. E.; Elstner, M.; Suhai, S.; Hobza, P. *J. Am. Chem. Soc.* **2002**, *124*, 3366.

(27) (a) Ren, J.; Chaires, J. B. *Biochemistry* **1999**, *38*, 16067. (b) Chaires, J. B. *Top. Curr. Chem.* **2005**, *253*, 33.

(28) (a) Wilson, W. D.; Tanious, F. A.; Mizan, S.; Yao, S.; Kiselyov, A. S.; Zon, G.; Strekowski, L. *Biochemistry* **1993**, *32*, 10614. (b) Strekowski, L.; Hojjat, M.; Wolinska, E.; Parker, A. N.; Paliakov, E. P.; Gorecki, T.; Tanious, F. A.; Wilson, W. D. *Bioorg. Med. Chem. Lett.* **2005**, *15*, 1097.

(29) Granzhan, A.; Ihmels, H. *ChemBioChem* **2006**, *7*, 1031.

observation that the tricyclic benzo[*b*]quinolizinium (**9**) does not significantly stabilize triplex DNA (cf. Supporting Information).

Conclusion

In summary, we present a comparative study of the DNA-binding properties of two isomeric dibenzoquinolizinium derivatives. Although the overall area of the π system of quinolizinium ions **5a** and **6** is of comparable size, the different shapes of the two isomers result in different DNA-binding properties. Both compounds intercalate into double-stranded DNA with large binding constants that are comparable to the ones reported for coralyne (**1**), a well-known tetracyclic intercalator with dibenzoquinolizinium structure. Notably, the stabilization of the DNA double helix toward dissociation is more pronounced upon association with **6** as compared to **5a**, the former being comparable to the one by coralyne (**1**). The CD spectroscopic data and molecular modeling studies of the ligand−DNA complex reveal a binding mode of **6** with DNA in which one-half of the molecule intercalates in the binding site and the other half of the molecule points inside the groove. In contrast, isomer **5a** is intercalated with its long molecular axes perpendicular to the long axis of the binding pocket.

In each of the binding modes of **5a** and **6**, a significant part of the molecule is accommodated in the groove next to the intercalation binding site. These aromatic moieties provide connection points for ternary complexes, such as with triplex DNA. Most notably, however, the quinolizinium ions **5a** and **6** exhibit a remarkable difference with respect to their ability to bind to triple-helical DNA and to stabilize the triplex upon association. Interestingly, the derivative **5a** exhibits a higher selectivity toward binding to the triplex DNA than **6**, as shown by the competition-dialysis method, whereas the stabilization of the triplex is more pronounced for the dibenzoquinolizinium **6** than for **5a**. Both properties need to be considered for possible applications of these compounds. In any case, for the design of duplex- or triplex-targeting drugs, both dibenzoquinolizinium ions **5a** and **6** as well as derivatives thereof may serve as promising lead structures. Nevertheless, a major drawback of the linear dibenzoquinolizinium **5a** is its dimerization and thermal decomposition. Thus, additional donor substituents, such as in **5b**, may be necessary to provide sufficient persistence of the compound.

Experimental Section

UV−Vis and Fluorescence Spectroscopy. DNA titration experiments were carried out in phosphate buffer (pH = 7.0; T = 25 °C, 10 mM, from K_2HPO_4 and KH_2PO_4). To a constant volume of an aqueous solution of the corresponding quinolizinium salt with a given concentration were added small amounts of DNA solution containing the same concentration of the ligand during titration. In general, titrations were performed according to published procedures,[6] and the resulting Scatchard plot[30] was analyzed by the method of McGhee and von Hippel[22] to obtain the intrinsic binding constant (K) and the binding-site size (n) in bases.

Flow Linear Dichroism. Linear dichroism (LD) spectra were recorded in a flow cell. The determination and interpretation of the data were performed as previously described.[23] DNA concentration was 2.27 mM in bases, and the measurements were performed at ligand-to-DNA ratios of 0.0, 0.08, and 0.2.

(30) Scatchard, G. *Ann. N.Y. Acad. Sci.* **1949**, *51*, 660.

DNA Melting Studies. DNA melting curves were performed according to published procedure.[29]

Competition-Dialysis Assay. The reduced assay was performed by a modification of the original method established by Chaires et al.[31] All dialysis experiments were performed using aqueous BPES buffer (6 mM Na_2HPO_4, 2 mM NaH_2PO_4, 1 mM Na_2EDTA, 185 mM NaCl, pH 7.0). For each dialysis assay, 400 mL of the 1 μM ligand solution was placed into a beaker. Six various DNA samples (1000 μL at a concentration of 75 μM monomeric unit) were placed into separate dialysis tubes. All six tubes were then placed into the beaker containing the ligand solution and dialyzed with continuous stirring for 24 h at room temperature and light exclusion. After 24 h, aliquots of DNA samples (900 μL) were taken from the dialysis tubes and placed into Eppendorf vials. Sodium dodecyl sulfate (SDS; 100 μL of 10% w/v solution, final concentration 1%) was added, and samples were mixed thoroughly. The total ligand concentration within each dialysis tube (c_t) was determined spectrophotometrically, using the calibration curve constructed for each ligand. The free ligand concentration (c_f) was determined using an aliquot of the dialysate solution, following the same procedure. The amount of bound ligand was determined by the difference, $c_b = c_t - c_f$, and plotted as a bar graph. For the calibration curves, samples with known concentrations of the ligand in the presence of 1% SDS were produced to determine the extinction coefficients of the ligands.

3-(1,3-Dioxolan-2-yl)isoquinoline (7). A solution of isoquinoline-3-carbaldehyde[32] (1.80 g, 11.4 mmol), ethane-1,2-diol (1.3 mL, 22.9 mmol), and *p*-TsOH (725 mg, 3.81 mmol) in toluene (50 mL) was heated under reflux in a Dean−Stark apparatus for 24 h. The reaction mixture was cooled to room temperature, and a saturated aqueous solution of Na_2CO_3 was added. The organic layer was separated, and the aqueous phase was extracted with Et_2O (3 × 50 mL). The combined organic phases were washed with water (3 × 70 mL) and dried with Na_2SO_4. The solvent was removed in vacuo to give **7** (2.24 g, 11.1 mmol, 97%) as a brown liquid: ^{1}H NMR ($CDCl_3$, 200 MHz) δ 4.12−4.19 (m, 2 H), 4.21−4.26 (m, 2 H), 6.09 (s, 1 H), 7.83 (d, 2 H, ^3J = 8 Hz, Ar−H), 7.63−7.76 (m, 3 H, Ar−H), 8.02 (dd, 1 H, ^3J = 8 Hz, ^4J = 1 Hz, Ar−H, Ar−H), 9.30 (s, 1 H, Ar−H); ^{13}C NMR ($CDCl_3$, 100 MHz) δ 72.7 (2 CH_2), 114.5 (CH), 118.9 (CH), 125.6 (CH), 125.9 (CH), 126.5 (C_q), 126.8 (CH), 129.9 (CH), 135.4 (C_q), 151.4 (CH), 152.0 (C_q). Anal. Calcd for $C_{12}H_{11}NO_2$ (201.22): C, 71.63; H, 5.51; N, 6.96. Found: C, 71.16; H, 5.65; N, 6.96.

2-Benzyl-3-(1,3-dioxolan-2-yl)isoquinolinium bromide [8(Br)]. Under argon gas atmosphere, a solution of 3-(1,3-dioxolan-2-yl)-isoquinoline (**7**) (1.00 g, 4.97 mmol) and benzylbromide (0.60 mL, 4.97 mmol) in DMSO was stirred for 7 days at room temperature. The solution turned to a dark brown oil and was added to ethyl acetate (2:l) with thorough stirring. A white solid precipitated, which was filtered off and washed three times with ethyl acetate to give **8(Br)** (1.45 g, 3.90 mmol, 79%) as a white solid: mp 150−151 °C; ^{1}H NMR (MeOH-d_4, 400 MHz) δ 4.20−4.27 (m, 4 H), 6.22 (s, 2 H), 7.37−7.39 (m, 2 H, Ar−H), 7.45−7.48 (m, 2 H, Ar−H), 8.09 (td, ^3J = 8 Hz, ^4J = 1 Hz, 1 H, Ar−H), 8.30 (td, ^3J = 8 Hz, ^4J = 1 Hz, 1 H, Ar−H), 8.40 (d, ^3J = 8 Hz, 1 H, Ar−H), 8.53 (d, ^3J = 8 Hz, 1 H, Ar−H), 8.79 (s, 1 H, Ar−H), 9.95 (s, 1 H, Ar−H); ^{13}C NMR (MeOH-d_4, 100 MHz) δ 62.3 (CH_2), 67.1 (CH_2), 99.2 (CH), 125.9 (CH), 129.0 (C_q), 129.1 (CH), 129.3 (C_q), 130.6 (CH), 130.7 (CH), 131.8 (CH), 133.2 (CH), 134.5 (C_q), 139.2 (CH), 139.5 (C_q), 143.9 (C_q), 153.8 (CH). MS (ESI): m/z (% relative intensity) 292 (M^+, 100). Anal. Calcd for $C_{19}H_{18}BrNO_2$ (372.26): C, 61.30; H, 4.87; N, 3.76. Found: C, 61.71; H, 4.79; N, 3.74.

2-Benzyl-3-(1,3-dioxolan-2-yl)-isoquinolinium tetrafluoroborate [8(BF$_4$)]. To a solution of **8(Br)** (100 mg, 269 μmol) in H_2O

(31) Chaires, J. B. In *Current Protocols in Nucleic Acid Chemistry*; Beaucage, S. L., Bergstrom, D. E., Glick, D., Jones, R. A., Eds.; Wiley-VCH: Weinheim, Germany, 2002.

(32) Teague, C. E.; Roe, A. *J. Am. Chem. Soc.* **1951**, *73*, 689.

(5 mL) was added slowly 48% aqueous HBF_4. A white powder precipitated, which was filtered off after 1 h to give **8(BF$_4$)** (94.0 mg, 247 μmol, 92%) as a white solid: mp 148−150 °C. Anal. Calcd for $C_{20}H_{20}BF_4NO_2$ (379.16): C, 60.19; H, 4.79; N, 3.69. Found: C, 59.82; H, 4.57; N, 3.65.

***anti*-Head-to-Head Dimer of Dibenzo[*b,g*]quinoliziniumbromide [ahh-(5a)$_2$].** A solution of **8(Br)** (500 mg, 1.34 mmol) in aqueous HBr (48%, 5 mL) was heated under reflux for 12 h. The solution was cooled to room temperature, and the yellow solution was carefully poured in THF (500 mL) with thorough stirring. A white solid precipitated that was separated by filtration to give the dimer **ahh-(5a)$_2$** (416 mg, 1.34 mmol, >97%) as a pale yellow solid: mp 251−252 °C; ^{1}H NMR (DMSO-d_6, 400 MHz) δ 6.02 (s, 2 H, CH, H12), 7.04 (td, ^3J = 15 Hz, ^4J = 8 Hz, ^5J = 1 Hz, 2 H, Ar−H, H2), 7.13 (td, ^3J = 15 Hz, ^4J = 8 Hz, ^5J = 1 Hz, 2 H, Ar−H, H3), 7.43 (d, ^3J = 7 Hz, 2H, Ar−H, H1), 7.51 (s, 2 H, CH, H5), 7.58 (d, ^3J = 7 Hz, 2 H, Ar−H, H4), 8.03−7.99 (m, 2H, Ar−H, H9), 8.22−8.21 (m, 4H, Ar−H, H7/H10), 8.39 (d, 2H, ^3J = 8 Hz, Ar−H, H8), 8.50 (s, 2 H, Ar−H, H11), 10.41 (s, 2 H, Ar−H, H6); ^{13}C NMR (DMSO-d_6, 100 MHz) δ 48.7 (CH, C12), 72.1 (CH, C5), 125.0 (C_q, C11a), 125.1 (CH, C11), 127.1 (CH, C10), 128.1 (CH, C1/2), 128.4 (CH, C4), 130.1 (CH, C3), 130.7 (CH, C8), 131.5 (CH, C9), 132.1 (C_q, C4a), 135.4 (C_q, C12a), 137.1 (C_q, C6a), 138.2 (CH, C7), 143.3 (C_q, C10a), 151.7 (CH, C6). MS (ESI): *m*/*z* (% relative intensity) 464 (M^+, 5), 257 (100). Anal. Calcd for $C_{34}H_{24}Br_2N_2 \cdot 2.5H_2O$ (664.36): C, 61.47; H, 4.40; N, 4.22. Found: C, 61.84; H, 4.39; N, 4.41.

Dibenzo[*b,g*]quinolizinium tetrafluoroborate [5a(BF$_4$)]. At 90 °C, **8(BF$_4$)** (161 mg, 488 μmol) was added in small portions to 2 g of polyphosphoric acid (84%, 2 g) and stirred for 20 min at 90 °C. Water (10 mL) was added carefully to the hot yellow solution (CAUTION: The addition of water may lead to a spontaneous strong boiling of the solution), and the solution was stirred for an additional 20 min at 90 °C. After cooling the solution to room temperature, a red solid precipitated, which was filtered off to give **5a(BF$_4$)** (113 mg, 356 μmol, 73%): mp ≥190 °C (decomp.); ^{1}H NMR (D_2O, 400 MHz) δ 7.62−7.80 (m, 4 H, Ar−H), 8.02 (d, ^3J = 8 Hz, 2 H, Ar−H), 8.11 (d, ^3J = 8 Hz, 2 H, Ar−H), 8.99 (s, 2 H, Ar−H), 9.92 (s, 2 H, Ar−H); ^{13}C NMR (MeOD, 100 MHz; because of the low solubility of the tetrafluoroborate, the counterion was exchanged by hydrogensulfate) δ 126.0 (CH), 127.7 (CH), 127.9 (C_q), 128.1 (CH), 131.9 (CH), 133.6 (CH), 134.9 (C_q), 136.0 (CH), 136.5 (C_q).

Photocleavage of the Dimer: To a solution of the dimer **ahh-(5a)$_2$** (6.31 mg, 10 μmol) in MeCN or H_2O (10.0 mL) was added 1-methoxynaphthalene (3.0 μL, 20 μmol). The mixture was shaken well until all of the dimer was dissolved. Subsequently, oxygen was removed by bubbling argon gas through the solution for 30 min. The solution was irradiated (λ = 350 nm) with a Rayonet photoreactor at room temperature for 40 s. The formation of the monomer was monitored by absorption spectroscopy. When the reaction was performed in water, excess 1-methoxynaphthalene was removed by extraction with CH_2Cl_2 (3 × 1 mL).

Computational Methodologies: All modeling studies were carried out on a 10 CPU linux cluster running under openMosix architecture.

Dibenzoquinolizinium ion structures were optimized using Hartree−Fock calculations with the 6-311++G(d,p) basis set. Quantum chemistry calculations were carried out with Gaussian 98.[33] Harmonic vibrational frequencies were obtained from RHF/6-311++G(d,p) calculations and used to characterize local energy minima (all frequencies real). Atomic charges were calculated by fitting to electrostatic potential maps (CHELPG method).[33]

The present study involved the use of consensus dinucleotide intercalation geometries d(ApT) and d(GpC) initially obtained using NAMOT2 (Nucleic Acid MOdeling Tool, Los Alamos National Laboratory, Los Alamos, New Mexico) software.[34] The d(ApT) and d(GpC) intercalation sites were contained in the center of a decanucleotide duplex of sequences d(5′-ATATA-3′)$_2$ and d(5′-GCGCG-3′)$_2$, respectively. Decamers in B-form were built using the "DNA Builder" module of Molecular Operation Environment (MOE, version 2005.06).[35] Decanucleotides were minimized using Amber94 all-atom force field,[36] implemented by MOE modeling package, until the root mean square (rms) value of the Truncated Newton method (TN) was <0.001 kcal mol^{-1} Å^{-1}. The dielectric constant was assumed to be distance independent with a magnitude of 4. Dibenzoquinolizinium ions **5a**−**6** were docked into both intercalation sites using flexible MOE-Dock methodology. The purpose of MOE-Dock is to search for favorable binding configurations between a small, flexible ligand and a rigid macromolecular target. Searching is conducted within a user-specified 3D docking box, using the "tabù search" protocol[37] and MMFF94 force field.[38] Charges for dibenzoquinolizinium ion structures were imported from the Gaussian output files. MOE-Dock performs a user-specified number of independent docking runs (55 in the presented case) and writes the resulting conformations and their energies to a molecular database file. The resulting DNA−dibenzoquinolizinium complexes were subjected to MMFF94 all-atom energy minimization until the rms of the conjugate gradient was <0.1 kcal mol^{-1} Å^{-1}. To model the effects of solvent more directly, a set of electrostatic interaction corrections were used. MOE suite implemented a modified version of GB/SA contact function described by Still and co-authors.[13,39] These terms model the electrostatic contribution to the free energy of solvation in a continuum solvent model. The interaction energy values were calculated as the energy of the complex minus the energy of the ligand, minus the energy of DNA: $\Delta E_{inter} = E_{(complex)} - (E_{(L)} + E_{(rDNA)})$.

Acknowledgment. This paper is dedicated to Prof. Manfred Christl, University of Würzburg, on the occasion of his 65th birthday. This work was generously financed by the Deutsche Forschungsgemeinschaft and the Fonds der Chemischen Industrie. The molecular modeling work coordinated by S.M. has been carried out with financial support from the University of Padova, Italy, and the Italian Ministry for University and Research (MIUR), Rome, Italy. S.M. is also very grateful to Chemical Computing Group for the scientific and technical partnership. We thank Anton Granzhan for discussions about triplex-binding ligands and the calculation of the transition dipole moments of **5a** and **6**.

(33) Frisch, M.; Trucks, G. W.; Schlegel, H.; Scuseria, G.; Robb, M.; Cheeseman, J.; Zakrzewski, V.; Montgomery, J.; Stratmann, R. E.; Burant, J. C.; Dapprich, S.; Millam, J.; Daniels, A.; Kudin, K.; Strain, M.; Farkas, O.; Tomasi, J.; Barone, V.; Cossi, M.; Cammi, R.; Mennucci, B.; Pomelli, C.; Adamo, C.; Clifford, S.; Ochterski, J.; Petersson, G. A.; Ayala, P. Y.; Cui, Q.; Morokuma, K.; Malick, D. K.; Rabuck, A. D.; Raghavachari, K.; Foresman, J. B.; Cioslowski, J.; Ortiz, J. V.; Stefanov, B. B.; Liu, G.; Liashenko, A.; Piskorz, P.; Komaromi, I.; Gomperts, R.; Martin, R. L.; Fox, D. J.; Keith, T.; Al-Laham, M. A.; Peng, C. J.; Nanayakkara, A.; Gonzalez, C.; Challacombe, M.; Gill, P. M. W.; Johnson, B. G.; Chen, W.; Wong, M. W.; Andres, J. L.; Head-Gordon, M.; Replogle, E. S.; Pople, J. A. *Gaussian 98*, revision A.6; Gaussian, Inc.: Pittsburgh, PA, 1998.

(34) *NAMOT2* (*N*ucleic *A*cid *MO*deling *T*ool); Los Alamos National Laboratory: Los Alamos, NM.

(35) *MOE* (The Molecular Operating Environment), version 2005.06; software available from Chemical Computing Group Inc., 1010 Sherbrooke Street West, Suite 910, Montreal, Canada H3A 2R7 (http://www.chemcomp.com).

(36) Cornell, W. D.; Cieplak, P.; Bayly, C. I.; Gould, I. R.; Merz, K. M.; Ferguson, D. M.; Spellmeyer, D. C.; Fox, T.; Caldwell, J. W.; Kollman, P. A. *J. Am. Chem. Soc.* **1995**, *117*, 5179.

(37) Baxter, C. A.; Murray, C. W.; Clark, D. E.; Westhead, D. R.; Eldridge, M. D. *Proteins: Struct., Funct., Genet.* **1998**, *33*, 367.

(38) (a) Halgren, T. A. *J. Comput. Chem.* **1996**, *17*, 490. (b) Halgren, T. A. *J. Comput. Chem.* **1996**, *17*, 520. (c) Halgren, T. A. *J. Comput. Chem.* **1996**, *17*, 553. (d) Halgren, T. A. *J. Comput. Chem.* **1996**, *17*, 587. (e) Halgren, T. A.; Nachbar, R. *J. Comput. Chem.* **1996**, *17*, 616. (f) Halgren, T. A. *J. Comput. Chem.* **1999**, *20*, 720. (g) Halgren, T. A. *J. Comput. Chem.* **1999**, *20*, 730.

(39) Qiu, D.; Shenkin, S.; Hollinger, F. P.; Still, W. C. *J. Phys. Chem. A* **1997**, *101*, 3005.

Supporting Information Available: List of materials and general methods; NMR spectra of **ahh-(5a)$_2$** (^{1}H,^{1}H ROESY); spectrophotometric titrations of poly[dA-dT]-poly[dA-dT] and poly[dG-dC]-poly[dG-dC] to **5a(BF$_4$)** and **6**, along with the corresponding Scatchard plots; melting profiles of poly[dA-dT]-poly[dA-dT] in the presence of **5a** at different Na^+ concentrations; melting profiles of poly[dA-dT]-poly[dA-dT], ct DNA, and poly[dA]-poly[dT]$_2$ in the presence of **9**; bar graph plot of the dialysis experiments of **9**; temperature-dependent UV−vis spectra of **5a(BF$_4$)**; different views of the optimized geometry of the intercalation complexes as calculated from molecular modeling studies; superimposed absorption spectra of **5a**, **ahh-(5a)$_2$**, and 1-methoxynaphthalene; photocleavage experiments with a cutoff filter (λ > 335 nm); and time-dependent absorption spectra of **5a**. This material is available free of charge via the Internet at http://pubs.acs.org.

JO0612271